Title
Active focus stabilization for upright selective plane illumination microscopy

Journal
Optics Express, 23(11)

ISSN
1094-4087

Authors
Hedde, Per Niklas
Gratton, Enrico

Publication Date
2015-06-01

DOI
10.1364/oe.23.014707

Active focus stabilization for upright selective plane illumination microscopy

Per Niklas Hedde and Enrico Gratton*

Laboratory of Fluorescence Dynamics, Department of Biomedical Engineering, University of California, Irvine, CA, USA

*egratton22@gmail.com

Abstract: Due to its sectioning capability, large field of view, and minimal light exposure, selective plane illumination microscopy has become the preferred choice for 3D time lapse imaging. Single cells in a dish can be conveniently imaged using an upright/inverted configuration. However, for measurements on long time scales (hours to days), mechanical drift is a problem; especially for studies of mammalian cells that typically require heating to 37°C which causes a thermal gradient across the instrument. Since the light sheet diverges towards the edges of the field of view, such a drift leads to a decrease in axial resolution over time. Or, even worse, the specimen could move out of the imaging volume. Here, we present a simple, cost-effective way to stabilize the axial position using the microscope camera to track the sample position. Thereby, sample loss is prevented and an optimal axial resolution is maintained by keeping the sample at the position where the light sheet is at its thinnest. We demonstrate the virtue of our approach by measurements of the light sheet thickness and 3D time lapse imaging of a cell monolayer at physiological conditions.

OCIS codes: (170.2520) Fluorescence microscopy; (180.6900) Three-dimensional microscopy.

References and links

1. J. Huisken, J. Swoger, F. Del Bene, J. Wittbrodt, and E. H. K. Stelzer, "Optical sectioning deep inside live embryos by selective plane illumination microscopy," Science **305**(5686), 1007–1009 (2004).
2. T. A. Planchon, L. Gao, D. E. Milkie, M. W. Davidson, J. A. Galbraith, C. G. Galbraith, and E. Betzig, "Rapid three-dimensional isotropic imaging of living cells using Bessel beam plane illumination," Nat. Methods **8**(5), 417–423 (2011).
3. P. N. Hedde, M. Stakic, and E. Gratton, "Rapid measurement of molecular transport and interaction inside living cells using single plane illumination," Sci. Rep. **4**(7048), 7048 (2014).
4. U. Krzic, S. Gunther, T. E. Saunders, S. J. Streichan, and L. Hufnagel, "Multiview light-sheet microscope for rapid *in toto* imaging," Nat. Methods **9**(7), 730–733 (2012).
5. A. D. Edelstein, M. A. Tsuchida, N. Amodaj, H. Pinkard, R. D. Vale, and N. Stuurman, "Advanced methods of microscope control using μManager software," J. Biol. Methods **1**(2), 10 (2014).
6. N. O. Deakin and C. E. Turner, "Paxillin comes of age," J. Cell Sci. **121**(15), 2435–2444 (2008).
7. M. A. Digman, P. W. Wiseman, A. R. Horwitz, and E. Gratton, "Detecting protein complexes in living cells from laser scanning confocal image sequences by the cross correlation raster image spectroscopy method," Biophys. J. **96**(2), 707–716 (2009).
8. M. A. Digman, R. Dalal, A. F. Horwitz, and E. Gratton, "Mapping the number of molecules and brightness in the laser scanning microscope," Biophys. J. **94**(6), 2320–2332 (2008).
9. L. Lanzano, M. A. Digman, P. Fwu, H. Giral, M. Levi, and E. Gratton, "Nanometer-scale imaging by the modulation tracking method," J. Biophotonics **4**(6), 415–424 (2011).
10. E. Baumgart and U. Kubitscheck, "Scanned light sheet microscopy with confocal slit detection," Opt. Express **20**(19), 21805–21814 (2012).
11. T. A. Planchon, L. Gao, D. E. Milkie, M. W. Davidson, J. A. Galbraith, C. G. Galbraith, and E. Betzig, "Rapid three-dimensional isotropic imaging of living cells using Bessel beam plane illumination," Nat. Methods **8**(5), 417–423 (2011).
12. T. Vettenburg, H. I. C. Dalgarno, J. Nylk, C. Coll-Lladó, D. E. K. Ferrier, T. Čižmár, F. J. Gunn-Moore, and K. Dholakia, "Light-sheet microscopy using an Airy beam," Nat. Methods **11**(5), 541–544 (2014).
13. M. Friedrich, Q. Gan, V. Ermolayev, and G. S. Harms, "STED-SPIM: Stimulated emission depletion improves sheet illumination microscopy resolution," Biophys. J. **100**(8), L43–L45 (2011).

#237998 - $15.00 USD Received 13 Apr 2015; revised 20 May 2015; accepted 20 May 2015; published 27 May 2015

14. L. Gao, "Extend the field of view of selective plan illumination microscopy by tiling the excitation light sheet," Opt. Express **23**(5), 6102–6111 (2015).

1. Introduction

In recent years, selective plane illumination microscopy (SPIM) has become the most popular technique for 3D time lapse imaging of larger specimens (~1 mm) such as tissues and whole organisms. In SPIM, two objective lenses are arranged perpendicular to each other with one of the lenses injecting a thin sheet of light that illuminates the focal plane of the other lens. This confinement of the excitation to a single plane minimizes out-of-focus background and significantly reduces light exposure of the sample during 3D image acquisition. Additionally, wide field detection with a camera provides superior imaging speed. Usually, the sample is embedded in a small gel cylinder and imaged from the side [1]. For coverslip-based single cell imaging, however, an upright/inverted (uSPIM/iSPIM) configuration is preferred. In such a setup the two objective lenses dip into the sample dish from the top [2,3]. Also, imaging of subcellular structures typically requires a higher spatial resolution, i.e., a thinner light sheet. This can be achieved with an excitation lens of higher numerical aperture (NA). Yet, a tighter focus gives rise to an increased beam divergence resulting in a poor axial resolution towards the edges of the field of view. Surface-attached cells have a fairly low extension in axial direction, thus, the axial resolution can be optimized by positioning the sample plane close to the focal plane of the excitation lens. However, during imaging, mechanical drift can cause the sample to divert from its optimal position, or, worse, escape the field of view. This is especially a problem for long term experiments lasting several hours or even days. To make matters worse, long term imaging of mammalian cells typically requires maintaining the sample at a temperature of 37°C. The introduction of a thermal gradient by sample incubation gives rise to an increased mechanical drift. Commercially available focus stabilization solutions are designed for single-lens use with perpendicular orientation to the coverslip and are not applicable to an upright/inverted light sheet microscope. Here, we present an easy-to-implement active focus stabilization for upright/inverted light sheet microscopy that requires the addition of only a few, low-cost components.

2. Methods

2.1 Measuring the axial sample position

In an upright/inverted SPIM configuration, the perpendicularly arranged excitation and detection lenses dip into the sample dish at a 45° angle with respect to the sample plane. Thus, the excitation light sheet is reflected off the interface at the bottom of the imaging dish with the reflection being directed towards the detection lens. For fluorescence imaging, this reflection is undesired and blocked by a suitable emission filter. However, the reflected light can be used to image the light sheet, measure its thickness and help align the two objective lenses [4]. In a properly aligned system, a section of the light sheet will appear as a strip on the camera with its vertical position, s_j, proportional to the distance between sample dish and excitation/detection optics as shown in Fig. 1. Thus, the relative axial position of the sample, s_z, can be calculated from,

$$s_z = s_j \cdot \frac{a}{\sqrt{2} \cdot M}, \tag{1}$$

with camera pixel size, a, magnification of the detection lens, M, and a factor of $1/\sqrt{2}$ to account for the detection lens inclination of 45° with respect to the sample plane. Consequently, by imaging the light sheet at regular time intervals, e.g., between the acquisition of each 3D stack of a time series, mechanical drift can be detected and compensated for. To avoid interference with the fluorescence imaging process, a laser line different than the one used for fluorescence excitation can be selected; a wavelength that can

#237998 - $15.00 USD Received 13 Apr 2015; revised 20 May 2015; accepted 20 May 2015; published 27 May 2015

pass through the emission filter enables detection of the light sheet reflection. Alternatively, for refocusing, the emission filter could be replaced by a neutral density filter with a motorized filter wheel.

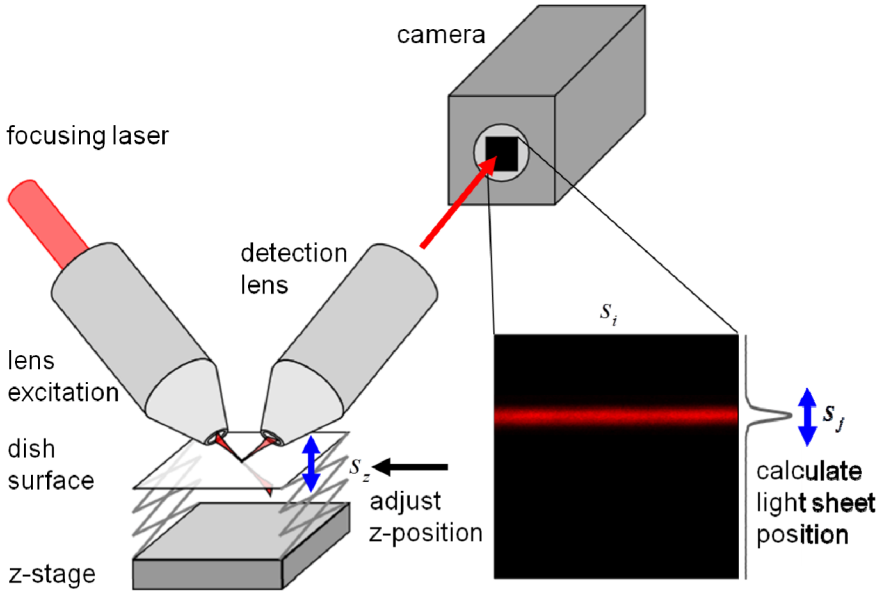

Fig. 1. Schematic of the active focus stabilization with camera-based detection. The light sheet is reflected off the bottom of the sample container and imaged onto the camera chip. From the position of the sheet on the image the z-position of the sample is calculated. Any displacement is corrected by moving the z-stage.

2.2 Description of the upright/inverted SPIM setup

A scheme of our home built upright/inverted SPIM setup is shown in Fig. 2. Three laser lines, a 488-nm laser diode (488nm, ISS, Champaign, IL, USA), a 561-nm solid state laser (CL561-150, CrystaLaser, Reno, NV, USA) and a 635-nm laser diode (CPS180, Thorlabs, Newton, NJ, USA) were combined via long pass dichroic mirrors. Laser lines were selected with an acousto optical tunable filter, AOTF, (AOTFnC-400.650, AA Opto-Electronic, Orsay, France). Note, however, that an AOTF is not mandatory and was simply used for convenience. For the focus stabilization presented here, laser switching on the millisecond timescale is sufficient which can be achieved by either direct modulation of the light source (diode lasers, many DPSS lasers) or by using mechanical shutters (gas lasers, fiber lasers, etc.). After single mode fiber (SMF) coupling, the light sheet was created by scanning the beam across the back focal plane of the excitation lens, OLE (CFI Plan Fluor 10XW, NA 0.3, Nikon, Melville, NY, USA). The scanning system includes a galvanometric mirror, GM (GVSM002, Thorlabs), a scan lens, SL (#49-356, Edmund Optics, Barrington, NJ, USA), and a tube lens, TLE (#49-362, Edmund Optics). To ensure homogeneous illumination of the focal plane of the detection objective, OLD (Scaleview 25x, NA 1.05, Olympus, Center Valley, PA, USA), the excitation lobe was scanned across the field of view once per exposure cycle. The corresponding voltage ramp was created with a function generator (DS345, SRS, Sunnyvale, CA, USA) synchronized to the camera and the amplitude matched to cover the field of view (291 µm). Alternatively, a cylindrical lens could be used to create the light sheet [1]. For simultaneous detection of GFP- and RFP-like fluorescence, collected light was spectrally separated by a long pass dichroic mirror (FF560, Semrock, Rochester, NY, USA) and cleaned with band pass filters, FR (605/70 ET, Chroma, Bellows Falls, VT, USA), and FG (FF03-525/50, Semrock). Both beams were imaged onto the opposing sides of a knife-edge prism mirror, PM (MRAK25-P01, Thorlabs), via tube lenses, TLDs (#47-740, Edmund

#237998 - $15.00 USD Received 13 Apr 2015; revised 20 May 2015; accepted 20 May 2015; published 27 May 2015

Optics). The channels were then re-imaged side-by-side onto the chip of a sCMOS camera (Zyla 4.2, Andor, Belfast, Ireland) with another lens LD (#47-737, Edmund Optics). The pixel size at the sample was 142 nm to accommodate the lateral resolution of the instrument of ~300 nm. Note that dual-channel detection was implemented for other experiments [3] and is not required for focus stabilization. The sample was positioned with a 3-axis stage (MAX343, Thorlabs). Control signals for both, laser switching and stage movement, were created with an Arduino board (Arduino Uno, arduino.cc). The sample was heated with a Peltier element. The temperature was stabilized with a heating controller (TC200, Thorlabs) coupled to a custom-built current amplifier and a PT-100 resistance temperature sensing element.

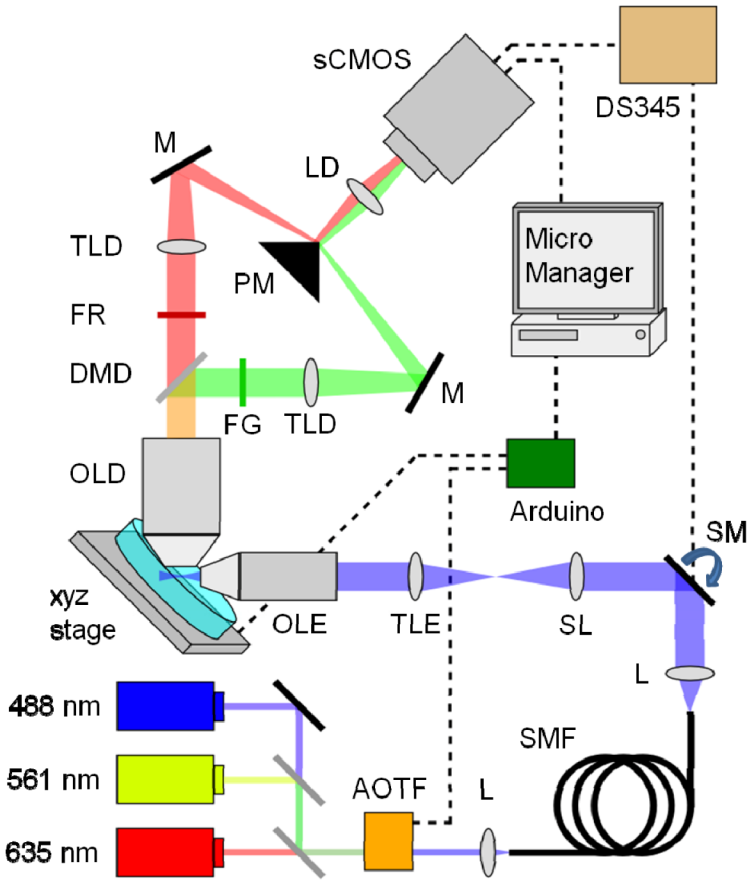

Fig. 2. Schematic of the upright/inverted SPIM setup. See main text for description.

2.3 Active feedback to correct the sample position

To run our SPIM system, we chose the freely available Micro-Manager open source microscopy software [5]. A custom beanshell script was written to manage 3D time lapse imaging including focus stabilization. In the experiments presented here, the 488-nm line was used for fluorescence excitation of GFP while the 635-nm line was utilized for monitoring of the light sheet. In the following, those two lasers are referred to as excitation and focusing lasers, respectively. A flowchart of the imaging procedure is shown in Fig. 3. Prior to starting the 3D image time series, the focusing laser was switched on and a reference image of the light sheet reflection was captured with the camera. From the camera image, the position of the maximum of the light sheet projection was calculated and stored as the reference sample position. This calculation was performed by the acquisition script within a few milliseconds.

#237998 - $15.00 USD Received 13 Apr 2015; revised 20 May 2015; accepted 20 May 2015; published 27 May 2015

Subsequently, the focusing laser was switched off and 3D time lapse imaging with the excitation laser was started. For imaging of rather flat samples, such as a monolayer of cells cultured in a dish, it is advantageous to move the sample in horizontal direction. This maximizes the field of view while keeping the sample close to the thinnest portion of the light sheet. To ensure the fastest possible acquisition of a stack, we typically moved the stage at a constant velocity with independently running acquisition. After completion of the stack, the sample was returned to the origin. To minimize photobleaching, the excitation laser was modulated with the camera exposure signal, a procedure often termed active blanking. After acquisition of each 3D stack of the time series, the light sheet reflection was captured again. The displacement from the original position was calculated, and the stage moved accordingly through communication of a TTL pulse train generated with the arduino board. Unfortunately, many motor stages including ours suffer from hysteresis if the direction of the movement is changed. A change in direction can occur since mechanical drift is not necessarily unidirectional. Hence, we repeated the focusing process until the sample displacement was less than a user defined threshold (here, 100 nm). A timeout was defined by the wait time between 3D stacks such that the following acquisition could not be missed.

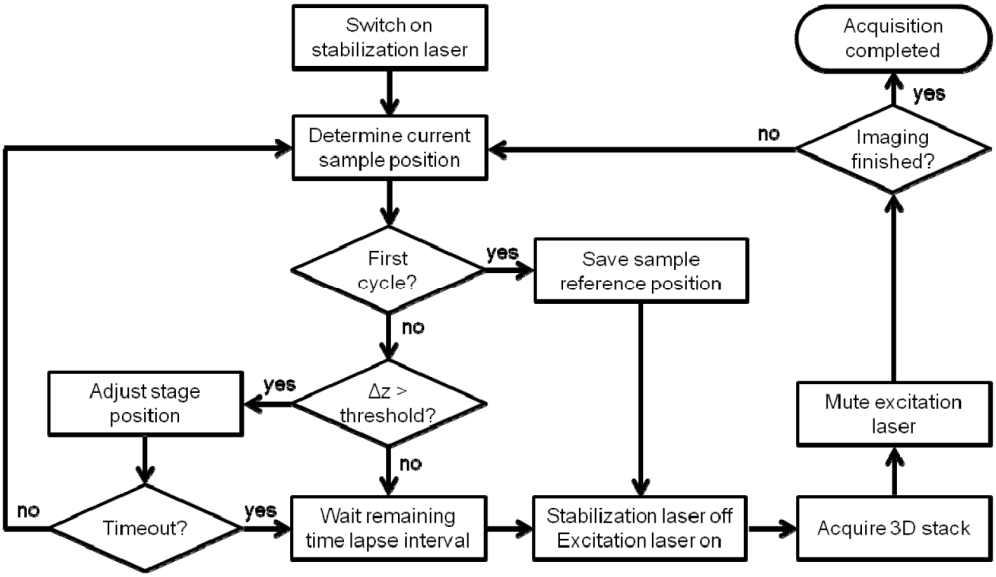

Fig. 3. Flowchart of the 3D time lapse acquisition procedure including focus stabilization. See main text for description.

3. Results

3.1 Active feedback performance evaluation

To evaluate the performance of our system, we imaged the light sheet for 18 h at 5 min time intervals both at room temperature (25°C) and at 37°C with and without active focus stabilization. Before taking the measurements, we allowed the system to equilibrate for 1 h. The intensity projection of the light sheet image, $I(s)$, was fitted with a Gaussian to determine its position, s_0, and width, w,

$$I(s) = I_{\text{offset}} + I_0 \cdot \exp\left(-\frac{2(s_j - s_0)^2}{w^2}\right), \tag{2}$$

#237998 - $15.00 USD Received 13 Apr 2015; revised 20 May 2015; accepted 20 May 2015; published 27 May 2015

with camera offset, I_{offset}, and light sheet amplitude, I_0. The position was converted from camera pixel to the actual stage displacement using Eq. (1). The sample position is plotted in Fig. 4(a) after subtraction of the initial position. Even at room temperature, a considerable drift was found spanning a quarter (24 µm) of the field of view in axial direction (103 µm) after 18 h. Consequently, the waist of the light sheet at the sample plane expanded from 1.3 µm to more than 5 µm as shown in Fig. 4(b). At 37°C, the same loss in axial resolution was detected after only 5 h, and, after 11 h, the drift covered almost half (46 µm) of the field of view. On the other hand, it is evident that this loss of axial resolution can be effectively prevented using active stabilization. The sample remained pinned down at the initial position and the light sheet waist at the sample plane stayed at its minimum of 1.3 µm.

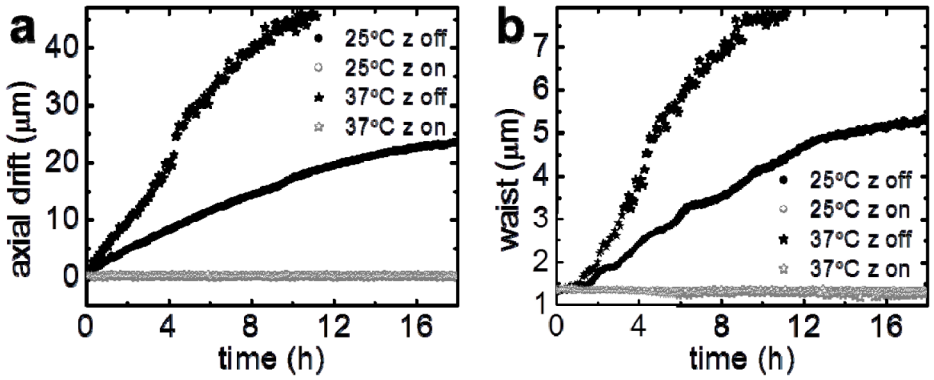

Fig. 4. (a) Measurements of the z-position of the sample without (solid symbols) and with active focus stabilization (open symbols) at 25°C (circular symbols) and 37°C (star symbols) over a period of 18 h. (b) Corresponding thickness ($1/e^2$ value) of the light sheet.

3.2 Active feedback during live cell imaging

To illustrate the impact of active feedback on image quality, we imaged CHO-K1 cells stably expressing EGFP-paxillin at physiological conditions (37°C, 5% CO_2). The Paxillin protein is vital for cell adhesion, cytoskeletal reorganization and cell migration [6]. It is recruited to focal adhesions of a cell from a pool of monomeric paxillin residing in the cell cytoplasm [7,8]. Figure 5 shows the 3D reconstructions of two samples imaged with (a,b) and without active stabilization (c,d). Based on the 0 h time point, the typical localization pattern of paxillin was observed for both samples. Adhesions were bright, crisp and very well distinguishable from cytoplasmic paxillin; clearly, there was no signal from the nucleus. After 5 h, the same pattern was found for the 3D reconstruction using active stabilization. However, without stabilization, a clear drift of the sample in axial direction was detected. The loss of axial resolution resulted in reduced image contrast. Consequently, in panel (d), it is very difficult to make out single adhesions. Also, the transition between cytoplasm and nucleus was washed out.

#237998 - $15.00 USD Received 13 Apr 2015; revised 20 May 2015; accepted 20 May 2015; published 27 May 2015

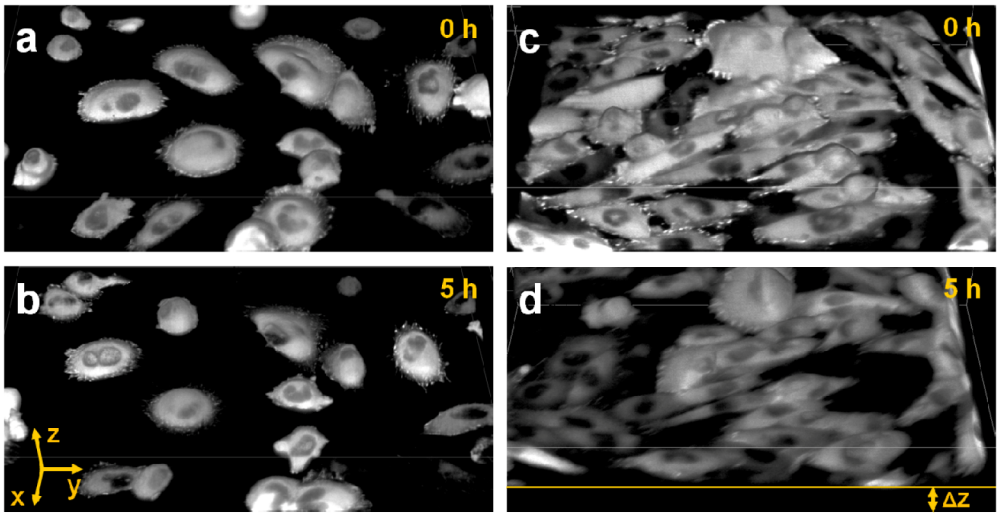

Fig. 5. 3D reconstruction of paxillin-EGFP expressing CHO-K1 cells at the indicated time points with (a,b) and without focus stabilization (c,d), both measured at 37°C. The axial displacement due to sample drift, Δz, is indicated in panel (d). Field of view, 178 × 252 × 32 μm^3 (xyz). The images were reconstructed using ImageJ 3D Viewer, voxels were painted with 50% transparency.

4. Discussion

Active feedback for focus control is a powerful addition to any imaging system. In laser scanning microscopy, for example, it has even been used to achieve super-resolution [9]. We have developed an easy-to-implement and cost-efficient method to actively stabilize the axial sample position in upright/inverted SPIM. Since the sample position is obtained through the existing optics of the system, only very few, if any, additional components are required. By keeping the light sheet focus close to the sample surface, axial resolution and image contrast are maximized during long term experiments. Additionally, maintaining the axial position prevents the specimen from drifting out of the field of view. And, especially, for a monolayer of cells the absence of sample drift allows to capture a thinner slice in the first place. This helps to minimize the amount of camera data created – a huge problem in light sheet microscopy. In principle, the precision could be enhanced by fitting a Gaussian to the light sheet image instead of determining the pixel position with maximum intensity. On the other hand, a fitting algorithm is computationally more intensive and will decrease feedback speed. Also, the increase in precision is not required for standard applications. In our setup, for example, a shift of one camera pixel corresponds to an axial displacement of 100 nm, much less than the axial resolution (1.3 µm) and close to the position resolution of the stage itself (60 nm). Yet, if the sample position is maintained, the width of the reflection is a measure of the alignment between detection and excitation lens. Hence, a potential drift between those two lenses could also be compensated for. Our method works well because reflections from a monolayer of cells are negligible compared to the reflection at the glass/water interface. Potentially, thick, strongly scattering samples could distort the light sheet image resulting in a loss of precision [10]. Also, samples such as zebrafish embryos are typically embedded in a gel with no reflective surface nearby. However, for such experiments, usually a large region of interest (~1 mm) is imaged with an excitation lens of low NA. Consequently, the light sheet is less divergent and sample drift is not as critical in terms of losing spatial resolution. Alternatively, an independent focusing laser could be mounted parallel to the objective lens and its reflection detected with a quadrant photo diode connected to the stage controller via a feedback loop. Such a hardware-based configuration would also allow for faster feedback than our software-based approach. Yet, it is more complicated to install, especially in a

#237998 - $15.00 USD Received 13 Apr 2015; revised 20 May 2015; accepted 20 May 2015; published 27 May 2015

commercial SPIM system. Also, the mounting position of focusing laser and detector must be carefully chosen, otherwise the function could be compromised by secondary drift of the mount. Our method does not suffer from such problems since it uses the same optics as used for fluorescence imaging. Recently, efforts have been made to reduce the divergence of the light sheet in general. These techniques include the application of advanced beam patterns such as Bessel beam [11] and Airy beam illumination [12], or even stimulated emission depletion [13]. Another possibility is to shift the light sheet focus across the image, at the expense of slowing down the acquisition process [14]. Yet, beam divergence is always present due to imperfections in optics and beam patterns. And active focus stabilization can still be applied to further improve image quality.

Acknowledgment

This work was supported by the National Institutes of Health (NIH)-P41 GM103540 and the NIH-P50 GM076516 grants. Also, we would like to thank Milka Stakic for cell culturing.

#237998 - $15.00 USD Received 13 Apr 2015; revised 20 May 2015; accepted 20 May 2015; published 27 May 2015